PROCEEDINGS OF THE INTERNATIONAL CONFERENCE NANOMATERIALS: APPLICATIONS AND PROPERTIES
Vol. **2** No 3, 03NCNN09(5pp) (2013)

The Formation of the Intermetallic-Containing Pd_2Sn Alloy: The Creation of the Isolated Adsorption Sites

E. Esmaeili[1,2,3,*], A.M. Rashidi[3], A.A. Khodadadi[2], Y. Mortazavi[2], M. Rashidzadeh[3]

[1] *Birjand University of Technology, Department of Chemical Engineering, P.O. Box: 97175/569, Birjand, Iran*
[2] *Catalysis and Nanostructured Materials Research Laboratory, School of Chemical Engineering, University of Tehran, Tehran, Iran*
[3] *Research Institute of petroleum industry (RIPI), West Blvd. Azadi Sport Complex, P. O. Box: 14665-1998, Tehran, Iran*

(Received 5 May 2013; published online 29 August 2013)

In the current study, tin-promoted Pd / MWNTs synthesized via polyol process were developed. TEM images evidences resulted in the formation of highly-dispersed Pd-Sn nanoparticles. The formation of Pd_2Sn structural phase was confirmed by XRD and TPR techniques, composed mainly of intermetallic species, supported by XPS results. In this research, we applied intermetallic-containing tin-promoted catalysts for the selective hydrogenation reaction of acetylene as the case study. The presence of a discontinuity in the Arrhenius plots could come from the kinetic factor as a result of change in acetylene coverage on Pd metallic ensembles. The intermetallic-containing assembled catalysts led to the good management of catalytic performance due to the creation of isolated adsorption sites on the catalyst surface, resulting in the higher ethylene selectivity.

Keywords: Polyol process technique, Intermetallic compounds, Geometric and electronic effects, Isolated adsorption sites.

PACS numbers: 71.20.Lp, 82.65. + r

1. INTRODUCTION

The use of ordered intermetallic compounds as catalysts in a variety of different reactions is generally investigated. However, the major contribution of these documents fails to disclose the application of this type of compounds to hydrogenations, let alone selective hydrogenations. In fact, the focus is on their use in fuel cells. Recently, Kovnir et al. [1] discovered the potential of these materials as highly-selective catalysts for the acetylene partial hydrogenation.

There are several reports regarding the positive effect of distinctive adsorption sites as isolated form on ethylene selectivity [2-5], in the course of acetylene hydrogenation. The formation of isolated adsorption sites could be occurred on the catalyst surface due to the creation of intermetallic compounds [2-3]. As known, these compounds have a well-defined homogeneous distribution of the active sites with a specified crystal structure because of the covalent bonding between the transition metals and the promoter applied [2]. Kovnir et al. [2-3] applied some kinds of Pd-Ga compound in the selective hydrogenation reaction of acetylene. They observed that the ethylene selectivity and the life time of the catalyst were improved.

Some hydrogenation promoters such as Ag [6-7], Ti [8-9], Ni [10], Au [11], Si [12] and Ga [13] in acetylene hydrogenation reaction have been utilized. Tin promoter is usually used in dehydrogenation reactions; however, there are some reports on its application in hydrogenation reaction as well [14-15]. The specific properties of Sn are usually interpreted in terms of an enhancing strong metal-support interaction linked to the alloy formation between Pd and Sn, leading to an altered noble metal-like electronic structure with respect to pure Pd [16].

According to Pisduangdaw et al. [17], the role of Sn in Pt-Sn catalyst is explained in terms of geometric and / or electronic effects. In geometric effects, tin decreases the size of platinum ensembles, which results in lower coke formation and in electronic effects, tin modifies the electronic density of Pt due to both positive charge transfer from Sn^{n+} species to Pt and the formation of different alloys of Pt-Sn. These modifications may be responsible for some changes in the heat of adsorption of different adsorbates, participating in the reaction.

In the present study, the main aim is to enhance the number of the isolated adsorption sites to design an efficient MWNTs-supported catalyst used in the catalytic reactions (herein, the case study is considered to be selective hydrogenation of acetylene).

2. MATERIAS AND METHODS

Carbon nanotubes were prepared by a chemical vapor deposition (CVD) of methane over Co-Mo / MgO at 900 °C [18], followed by washing in an aqueous solution of HCl and then, in HNO_3 solution to eliminate all the impurities. Afterwards, the resulted MWNTs were functionalized under sonication for 3 h in a mixture of sulfuric and nitric acids with volumetric ratio of 3 : 1, respectively.

All the catalysts in this study were prepared by polyol-based method, according to the recipe reported in the literature [19-20]. In this method, MWNTs were dispersed in ethylene glycol (EG, Merck) and sonicated for 30 min. An aqueous solution of metal precursors ($PdCl_2$, $SnCl_2.2H_2O$, Merck) was then added slowly to this solution under vigorous stirring, followed by pH adjustment

* esmaeili@birjandut.ac.ir

at about 12. The solution was rapidly heated up to 140 °C under reflux condition, while argon gas (30 cc/min) was passed through it. The reaction mixture was held at this temperature for 3 h. Products were filtered and dried in a vacuum oven at 90 °C for 4 h. The molar ratios of Sn to Pd of 1 : 0.1, 0.25, 0.5, 1.0 and 0.1 wt % Pd loading for all of the samples were utilized, except for XRD and XPS analyses where the Pd loading of 5.0 wt % was utilized.

Catalytic activities of all the catalysts were carried out in a stainless steel vertical reactor of 1/4" outer diameter containing 0.1 g of catalyst powder diluted with SiC. The gas feedstock (H_2 : C_2H_2 = 2 : 1) diluted with Ar (70 vol %) was introduced into the reactor with GHSV of about 33000 h^{-1}. The reaction temperature was held in the range of 60-180 °C. To ensure the isothermal condition during the exothermic reaction, an oil bath, having a large thermal mass, was used. The outlet gas of the reactor was analyzed by a Shimadzu gas chromatography with an alumina packed column.

Transmission electron microscopy (TEM) images were obtained using a CM-FEG-Philips instrument operated with an accelerating voltage of 120 keV to investigate the dispersion and metal particle size of the catalysts. X-ray diffraction (XRD) with Cu Kα radiation source (Philips PW-1840) was used to study the crystalline phases of the catalysts and to obtain the average crystallite size of the nanoparticles (by Scherrer's equation). A Micrometrics TPD-TPR 2900 system was used to study the reduction behavior of the promoted and unprompted catalysts. X-ray photoelectron spectroscopy (XR3E2, 8025-BesTec) was applied to investigate the chemical states and the relative ratio of the elements on surface of the catalyst.

3. RESULTS AND DISCUSSION

TEM micrographs of MWNTs-supported tin-promoted Pd nanocatalysts are presented in Fig. 1, showing highly-dispersed nanoparticles. The size of nanoparticles is found to be less, for the catalyst with Sn to Pd molar ratio of 0.25, when it is compared with the ones of Sn / Pd = 1.

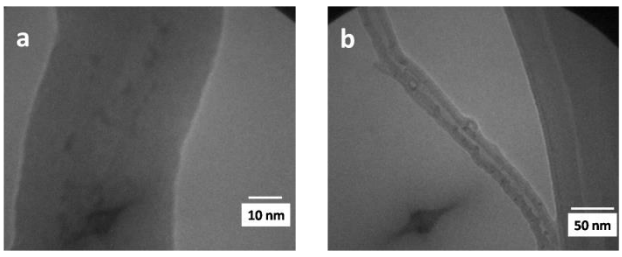

Fig. 1 – TEM micrographs of MWNTs-supported Pd promoted by Sn with a) Sn / Pd = 0.25 and b) Sn / Pd = 1

Since, the characterization of low palladium loading of all the catalysts, i.e. 0.1 wt %, using XRD and XPS is so difficult, we needed to increase the amount of Pd loading up to 5.0 wt %, in accordance with the literature [21]. Fig. 2 shows the XRD patterns of MWNTs-supported 5.0 wt % Pd tin-promoted catalysts.

The (111) crystallite plane of Pd appeared at the Bragg angle of 40.2 ° has been indicated by a vertical line in Fig. 2, however, some parts of Pd is in the oxide form, as shown in the figure. It is found that there is a slight shift in 2θ value for this plane, when Sn is added to Pd catalysts. This slight shift with respect to (111) plane of Pd reflection occurred at $2\theta = 39.49$ ° may be attributed to the formation of Pd_2Sn alloy, as described in JCPDS-ICCD data bank (Card No. 26-1297).

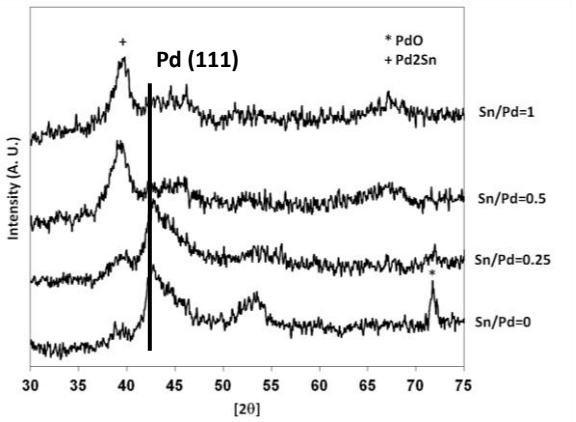

Fig. 2 – The XRD patterns of 5.0 wt % Pd catalysts, unpromoted and promoted with different molar ratios of Sn

The XPS results of 5.0 wt % Pd catalysts promoted by tin with Sn to Pd molar ratios of 0.25 and 1 are depicted in Fig. 3. According to Fig. 3a, three distinguished peaks associated with Sn $3d_{5/2}$ spectra are observed. The first one centered at about 485.2 eV is assigned to metallic tin (Sn^0), the second one, appeared at ca. 486.5 eV, is associated to Sn^{2+} species, forming Pd-Sn-O and / or Sn-O phases. The peak centroid at about 487.5 eV is related to the Sn^{4+} species, indicating the presence of the stoichiometric SnO_2 [22]. Fig. 5b exhibits the spectra of Pd $3d_{5/2}$ for the catalysts with Sn to Pd molar ratios of 0.25 and 1.

Table 1 illustrates the results of the relative percentage of surface species for the catalysts. Since, the presence of Pd_2Sn is confirmed by XRD diffraction peaks (Fig. 2), the stoichiometric value of 2 : 1 may be respectively assumed for the corresponding amounts of Pd:Sn. To calculate this ratio based on the results of XPS, the peak surface area of zero-valent tin is considered. According to Table 1, the ratio of Pd to Sn^0 on the surface is found to be 10.6 and 4.6, in accordance with the catalysts with Sn to Pd molar ratio of 0.25 and 1, respectively. Therefore, the smaller value of Pd:Sn is found for the catalyst with Sn to Pd molar ratio of 1, which is about 2 times of the stoichiometric value of 2, as mentioned before. Meanwhile, this ratio is more than 5 fold of the stoichiometric value for the catalyst with Sn / Pd = 0.25. This confirms that the Pd segregation is more pronounced for the catalyst promoted by tin to palladium molar ratio of 0.25 [23]. These findings could rationalize the presence of more Pd multiple bonded sites on the surface of the catalyst with tin to palladium molar ratio of 0.25. Considering the results presented in Fig. 3b, since full width at half maximum (FWHM) of the Pd peak is large (> 1.5 eV), the presence of more than one palladium species is expected [24]. According to this figure, the peaks related to Pd species are appeared at about 335.0 eV and 336.3 eV, in accordance with the

metallic palladium ensembles and Pd species due to the presence of Pd-Sn intermetallic compounds, respectively [2-3]. However, from Table 1, the percentage of Pd in intermetallic state is more significant for the catalyst with Sn to Pd molar ratio of 1 (70.8 % in contrast to 29.2 % in metallic form), in comparison with the catalyst with Sn / Pd = 0.25; i.e. 56.4 % in the intermetallic mode and 46.3% in the metallic state. As is established in the literature [2-3], the intermetallic compounds have intrinsically isolated adsorption sites, which differ from the Pd metallic ensembles.

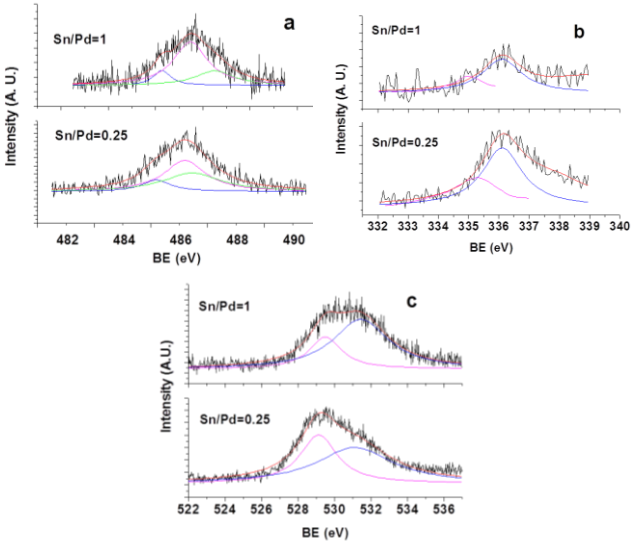

Fig. 3 – The results of a) Sn $3d_{5/2}$, b) Pd $3d_{5/2}$ and c) O1s binding energies of the catalysts with Sn to Pd molar ratios of 0.25 and 1

The O1s core level binding energies for the Sn-promoted Pd catalysts with Sn / Pd molar ratios of 0.25 and 1 are presented in Fig. 3c. The peak centroid at about 529.5 eV is indicative of the oxygen associated with Pd-Sn-O and / or Sn-O phases, followed by a shoulder at ca. 531.1 eV related to the oxygen of SnO_2 lattice [25]. Higher percentage of the oxygen associated with SnO_2 lattice for the catalyst with Sn to Pd molar ratio of 0.25 (28.0 %) compared to that of the sample with molar ratio of 1 (20.1 %) could be explained by the possibility of the destruction of Pd-Sn intermetallic compound, followed by the formation of SnO_2 [2]. In line with these findings, the presence of isolated adsorption sites on the catalyst surface with tin to Pd molar ratio of 1 is more considerable compared to the catalyst with tin to palladium molar ratio of 0.25.

Table 1 – The binding energies of Pd $3d_{5/2}$, Sn $3d_{5/2}$ and O1s and the relative percentage of surface species for the 5.0 wt % Pd catalysts promoted by Sn to Pd molar ratio of 0.25 and 1

Catalyst (Sn/Pd)	Pd/C	Sn^0/C	Pd/Sn^0
0.25	0.509	0.048	10.6
1	0.101	0.022	4.6

The plots for calculation of apparent activation energies for some of the samples are illustrated in Fig. 4. This figure implies the Arrhenius plot for the un-promoted Pd catalyst which is continuous in the entire temperature range examined. However, Fig. 4b shows a discontinuity in the plot for the tin-promoted catalyst (Sn / Pd = 1), i.e. two different activation energies for different temperature range. According to Fig. 4c, the value of activation energy for low temperature region (up to 100 °C) is evaluated to be 29.6 kJ/mol for Pd catalyst promoted by 0.25 molar ratio of Sn. The activation energy for the un-promoted Pd catalyst is 42.6 kJ/mol. These values are reasonably in a good agreement with those reported in the literature [5, 26] and comparable to activation energies for the reactions in kinetic controlled regime, i.e. the absence of mass transfer limitation.

The changes in activation energies with further addition of tin to Pd catalyst may be attributed to the alloy formation [26-27], different interactions between Pd and Sn and especially, varying the electron transfer from Sn to Pd d-bands [28].

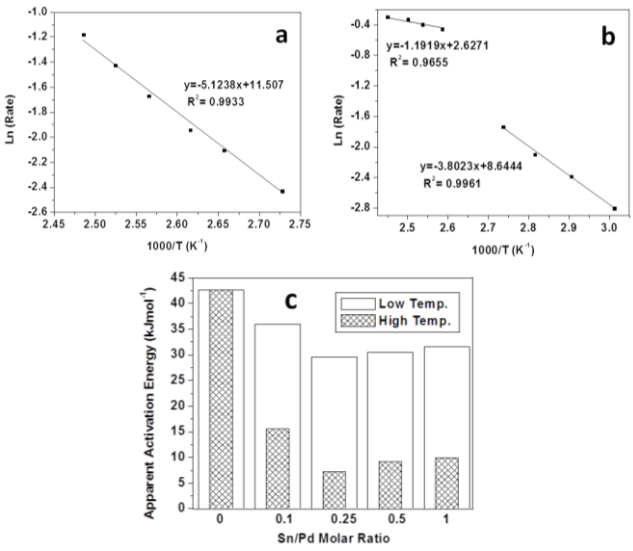

Fig. 4 – Arrhenius plots of a) Pd catalyst, b) Sn-promoted Pd catalyst with Sn / Pd = 1, c) apparent activation energies of Pd / MWNTs catalysts with different Sn / Pd ratios

Based on Fig. 4c, the highest value of activation energy belongs to the un-promoted Pd catalyst which may be explained by the filling of Pd d-band by electrons from the dissolved hydrogen atoms which causes an increase in activation energy. This explanation may be found as a result of Farkas's experiment during which he investigated the parahydrogen conversion on the inlet and outlet sides of a platinum disc and a platinum tube through which hydrogen was diffusing. He observed that the activation energy for the conversion of dissolved hydrogen atoms was higher on the side exposed to hydrogen than the other one [29].

According to some reports [29-30], the effect of dissolved hydrogen, especially, in the case of hydrogenation catalysts, is shown by an increase in activation energy which may be explained by the filling of the Pd *d*-vacancies by electrons from hydrogen β-hydride. Authors [29-30] believed that some traces of even oxygen or some alloying may lead to the activation of the catalysts through the discharge of dissolved hydrogen. Therefore, the addition of tin may help Pd to lose hydrogen *β*-hydride, leading to lower activation energy. Hence, a very sharp decrease of activation energy at 0.25 molar

ratio of Sn to Pd could be attributed to the loss of Pd β-hydrides as a result of electron transfer from tin to palladium. Since, there is no clear change in activation energy with further addition of Sn to Pd; one may conclude that there are not enough electrons to fill up Pd d-bands, as described in literature [29-30].

According to Figs. 4b and c, there is a discontinuity in activation energies for the low and high temperature regions with addition of Sn to Pd catalyst. Some authors observed the same behavior for hydrogenation of acetylene [5, 31-32]. Moyes et al. [31] attributed the discontinuous jumps in the Arrhenius plots to two different modes of acetylene molecules on the catalyst surface. Furthermore, McLeod et al. [5] obtained values of 15.9 and 61.9 kJ/mol for the apparent activation energy of acetylene hydrogenation reactions in the high- and low-activity regimes, respectively. Based on their assumptions, the presence of two distinct types of adsorption sites on the Pd metallic ensembles is possible, the former is assigned to the isolated one, whereas, the latter one is connected to other vacant sites. The density of these adsorption sites may depend on the acetylene coverage on the surface [5, 32].

As mentioned earlier, for intermetallic compounds, the isolated adsorption sites are the predominant sites which have no neighboring adsorption sites; therefore, the presence of just one mode of adsorbed acetylene is deduced. Meanwhile, the presence of both the isolated and the connected adsorption sites are possible upon the reaction as a result of the simultaneous presence of the intermetallic and / or Pd metallic ensembles. Therefore, according to the results presented in Fig. 4c, the creation of two modes of acetylene coverage on Pd metallic ensembles of Sn-promoted catalysts at low and high temperature regions, followed by changing the kinetic regimes is substantiated. A drastic decrease of apparent activation energy from 29.6 kJ/mol at lower temperature range to 7.2 kJ/mol at higher temperature one may be indicative of a change in acetylene coverage, as a result of the geometrical factors. In geometrical aspect, a decrease in particle size may originate from alloying, as illustrated previously (see Figs. 1 and 2). This effect is more pronounced for the catalyst with 0.25 molar ratio of Sn to Pd, leading to a sharp decrease in apparent activation energy.

The catalytic activities of tin-promoted and un-promoted catalysts at different temperatures are presented in Fig. 5. The temperature range for the start and completion of the reaction is very broad for the un-modified Pd catalyst. However, this temperature range becomes narrower for the tin-containing catalysts. Considering the results presented in Fig. 5, one could conclude that the reactivity of the catalysts improves upon addition of Sn to Pd molar ratios up to 0.25 (see inset of Fig. 5). According to the inset, there is a minimum value of the reaction temperature for the same acetylene conversion in the case of tin to palladium molar ratio of 0.25. For instance, the reaction temperature to obtain 50 and 90 % acetylene conversion, respectively, are 97.5 °C and 103 °C for the catalyst promoted with molar ratio of 0.25 of Sn to Pd, while, the corresponding temperatures are 133 °C and 148 °C, respectively, for the un-promoted Pd catalyst.

As found from TEM images and XRD patterns (Figs. 1 and 2), it may be expected that the simultaneous geometric and electronic effects for the Sn-promoted catalysts are involved in the catalytic performance. However, the electronic effect is more pronounced for the catalysts with the molar ratios of Sn to Pd up to 0.25.

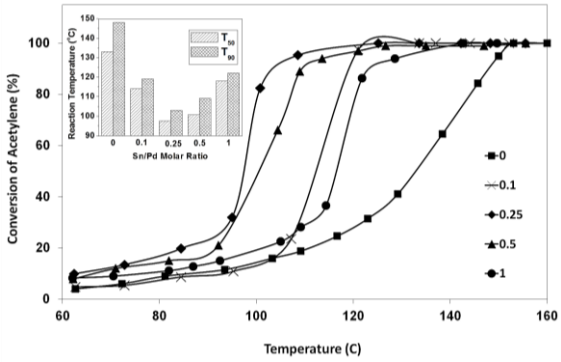

Fig. 5 – Acetylene conversion versus temperature on catalysts with different Sn : Pd ratios. Inset shows the temperature for 50 and 90 % of acetylene conversion versus Sn:Pd ratios

Fig. 6 demonstrates the selectivity to ethylene for the catalysts with different molar ratios of Sn to Pd. In the case of un-promoted Pd catalyst, the minimum selectivity to ethylene is about 69 % at ca. 60 °C, whereas, it reaches to 90.7 % by increasing the temperature up to 180 °C. Addition of Sn could increase ethylene selectivity, as with the molar ratio of Sn to Pd up to 1, the ethylene selectivity increases from 80.8 % at ca. 60 °C to about 96 % at 180 °C, respectively. According to some reports [4, 33-34], ethylene selectivity is improved with an increase in temperature. Molero et al. [26] observed a similar increase of ethylene selectivity with temperature, when they applied Pd foil as an acetylene hydrogenation catalyst. Furthermore, Mei et al. [34] observed an enhancement of ethylene selectivity by Monte Carlo simulation.

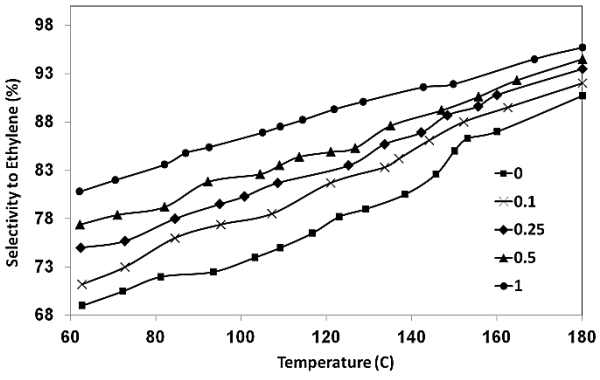

Fig. 6 – Effect of different Sn to Pd molar ratio on selectivity to ethylene and ethane at various temperatures (All catalysts contain 0.1 wt % Pd)

In several recent investigations [4-5], the high ethylene selectivity in acetylene hydrogenation reaction has been attributed to the presence of distinct adsorption sites within the carbonaceous overlayer which may be geometrically formed on the metal surface. Indeed, ac-

cording to McLeod et al. [5], higher selectivity to ethylene with increased temperature is attributed to the existence of more isolated adsorption sites compared to the sites which are connected to the neighboring sites. From Fig. 6, the existence of discontinuity in Arrhenius plots was ascribed to the changes in the acetylene coverage. According to Fig. 5 and Table 1, more intrinsically isolated adsorption sites on the catalyst surface was already confirmed by XPS analysis data (Fig. 5 and Table 1) for the tin-promoted catalyst with molar ratio of 1 (Sn / Pd = 1), when it is compared with the catalyst containing tin to palladium molar ratio of 0.25. According to Osswald et al. [23], the changes in the electronic structure of elemental Pd by the formation of Pd-included intermetallic compounds may enhance the ethylene selectivity through the creation of the isolated adsorption sites.

Considering Figs. 7 and 8, it is clear that both the conversion of acetylene and the selectivity to ethylene could be improved, as the temperature is increased. Therefore, it may be expected that larger number of isolated adsorption sites resulted from the presence of the intermetallic compounds, as non-competitive adsorption ones, are formed at higher temperatures which are responsible for enhancing the catalytic activity.

4. CONCLUSION

Pd-Sn nanoparticles supported on MWNTs were synthesized using a polyol technique, forming intermetallic species of Pd_2Sn alloy, confirmed by XRD patterns and XPS spectra. High-concentration acetylene feedstock was considered for further selective hydrogenation to ethylene using Pd-Sn intermetallic-containing catalysts.

A distinct discontinuity of Arrhenius plots for low and high temperature regions was observed for tin-promoted Pd catalysts, indicating significant changes in acetylene coverage on Pd metallic multiple-bonded sites and subsequently, the kinetic regime. It was rationalized that the presence of more isolated adsorption sites could be responsible for the increased selectivity to ethylene. The presence of intrinsically isolated adsorption sites originated from the intermetallic compounds was more pronounced for the catalyst with increased Sn to Pd molar ratios.

AKNOWLEDGEMENTS

The financial support for this research by Research Institute of Petroleum Industry (RIPI) is greatly appreciated.

REFERENCES

1. K. Kovnir. J. Osswald, M. Armbrüster, R. Giedigkeit, T. Ressler, Y. Grin, R. Schlögl, *Stud. Surf. Sci. Catal.* **162**, 481 (2006).
2. K. Kovnir, J. Osswald, M. Armbrüster, D. Teschner, G. Weinberg, U. Wild, A. Knop-Gericke, T. Ressler, Y. Grin, R. Schlögl, *J. Catal.* **264**, 93 (2009).
3. K. Kovnir, M. Armbrüster, D. Teschner, T.V. Venkov, F.C. Jentoft, A. Knop-Gericke, Y. Grin, R. Schlögl, *Sci. Technol. Adv. Mater.* **8**, 420 (2007).
4. A. Borodzinski, A. Golebiowski, *Langmuir* **13**, 883 (1997).
5. A.S. McLeod, R. Blackwell, *Chem. Eng. Sci.* **59**, 4715 (2004).
6. B. Ngamsom, N. Bogdanchikova, M. Avalos Borja, P. Praserthdam, *Catal. Commun.* **5**, 243 (2004).
7. Q. Zhang, J. Li, X. Liu, Q. Zhu, *Appl. Catal. A: Gen.* **197**, 221 (2000).
8. J. Panpranot, K. Kontapakdee, P. Praserthdam, *Appl. Catal. A: Gen.* **314**, 128 (2006).
9. J. Hong, W. Chu, M. Chen, X. Wang, T. Zhang, *Catal. Commun.* **8**, 593 (2007).
10. O. Mekasuwandumrong, N. Wongwaranon, J. Panpranot, P. Praserthdam, *Mater. Chem. Phys.* **111**, 431 (2008).
11. M.S. Chen, D.W. Goodman, *Catal. Today* **111**, 22 (2006).
12. E.W. Shin, J.H. Kang, W.J. Kim, J.D. Park, S.H. Moon, *Appl. Catal. A: Gen.* **223**, 161 (2002).
13. K. Kovnir, M. Armbruster, D. Teschner, T.V. Venkov, L. Szentmiklosi, F.C. Jentoft, A. Knop-Gericke, Y. Grin, R. Schlogl, *Surf. Sci.* **603**, 1784 (2009).
14. S. Sahoo, P.V. Rao, D. Rajeshwer, K.R. Krishnamurthy, I.D. Singh, *Appl. Catal. A: Gen.* **244**, 311 (2003).
15. E.L. Jablonski, A.A. Castro, O.A. Scelza, S.R. De-Miguel, *Appl. Catal. A: Gen.* **183**, 189 (1999).
16. H. Lorenz, Q. Zhao, S. Turner, O.I. Lebedev, G.V. Tendeloo, B. Klotzer, C. Rameshan, K. Pfaller, J. Konzett, S. Penner, *Appl. Catal. A: Gen.* **381**, 242 (2010).
17. S. Pisduangdaw, J. Panpranot, C. Methastidsook, C. Chaisuk, K. Faungnawakij, P. Praserthdam, O. Mekasuwandumrong, *Appl. Catal. A: Gen.* **370**, 1 (2009).
18. R. Arasteh, M. Masoumi, A.M. Rashidi, L. Moradi, V. Samimi, S.T. Mostafavi, *Appl. Surf. Sci.* **256**, 4447 (2010).
19. X. Yu, S. Ye, *J. Power Sources* **172**, 133 (2007).
20. H.S. Oh, J.G. Oh, Y.G. Hong, H. Kim, *Electrochim. Acta* **52**, 7285 (2007).
21. P. Praserthdam, B. Ngamsom, N. Bogdanchikova, S. Phatanasri, M. Pramotthana, *Appl. Catal. A: Gen.* **230**, 41 (2002).
22. J. Arana, P. Ramirez de la Piscina, J. Llorca, J. Sales, N. Homs, *Chem. Mater.* **10**, 1333 (1998).
23. J. Osswald, K. Kovnir, M. Armbruster, R. Giedigkeit, R.E. Jentoft, U. Wild, Y. Grin, R. Schlogl, *J. Catal.* **258**, 219 (2008).
24. A. Haghofer, K. Föttinger, F. Girgsdies, D. Teschner, A. Knop-Gericke, R. Schlögl, G. Rupprechter, *J. Catal.* **286**, 13 (2012).
25. N. Tsud, T. Skala, F. Sutara, K. Veltruska, V. Dudr, M. Yoshitake, K.C. Prince, V. Matolin, *J. Phys.: Condens. Matter.* **21**, 185011 (2009).
26. H. Molero, B.F. Bartlett, W.T. Tysoe, *J. Catal.* **181**, 49 (1999).
27. S. Azad, M. Kaltchev, D. Stacchiola, G. Wu, W.T. Tysoe, *J. Phys. Chem. B* **104**, 3107 (2000).
28. Y. Wang, J. Qu, R. Wu, P. Lei, *Water Res.* **40**, 1224 (2006).
29. A. Farkas, *Disc. Faraday Soc.* **32**, 1667 (1936).
30. A. Couper, D.D. Eley, *Disc. Faraday Soc.* **8**, 172 (1950).
31. R.B. Moyes, D.W. Walker, P.B. Wells, D.A. Whan, *Appl. Catal.* **55**, L5 (1989).
32. A.S. McLeod, L.F. Gladden, *J. Chem. Phys.* **110**, 4000 (1999).
33. H. Bazzazzadegan, M. Kazemeini, A.M. Rashidi, *Appl. Catal. A: Gen.* **399**, 184 (2011).
34. D. Mei, M. Neurock, C.M. Smith, *J. Catal.* **268**, 181 (2009).